Lasers in Manufacturing Conference 2019

The effects of weld parameters on fatigue strength of a pulsed laser welding Ni-base alloy thin sheet with filler wire

Jingling Yu[a], Jun Liu[a], Dongsheng Chai[a], Bo Cheng[a], Fangyong Niu[a], Guangyi Ma[a*], Dongjiang Wu[a]

[a]*Dalian University of Technology, Dalian, Liaoning Province, 116024, PR of China*

Abstract

Welded nickel-based alloy Hastelloy C-276 thin sheets were widely used in nuclear industry. The fatigue life of laser weld joints with filler wire has attracted considerable interest because of the cyclic loading caused by the working condition. In the present work, fatigue strength could be predicted by weld parameters with the help of Respond surface method (RSM) and Finite element method (FEM). The relationship of weld parameters and weld profile was established by RSM experiment. Changes in weld profile would lead to the different stress concentration effect which affect the fatigue strength most. The results showed that the weld joint has better fatigue strength when the weld geometry is symmetry. Weld speed has the most significant influence on fatigue strength, and has influence on optimization of other parameters. The risk of fatigue crack can be minimized by optimization of weld parameters.

Keywords: Hastelloy C-276, Laser weld with filler wire, Respond surface method, fatigue strength;

1. Introduction

The Ni-based Hastelloy C-276 alloy is widely used in chemical processing, the nuclear industry and marine engineering components such as pumps, valve parts and spray nozzles, due to its excellent resistance to corrosive environments and its superior mechanical properties [1-2]. Some nuclear pump parts are made of

* Corresponding author. Tel.: +86 15668680920;
E-mail address: gyma@dlut.edu.cn.

Hastelloy C-276 thin sheet via welding. while laser welding Hastelloy C-276 thin sheet without filler wire is likely to generate defects and undercuts with poor clamping and a gap width greater than 10% of sheet thickness. Therefore laser welding with filler wire is applied although stress concentration is invited around the weld toe. The nuclear parts were bearing alternative loading in working condition. Thus the fatigue strength of the weld joint especially the critical area around weld toe should be evaluated.

The fatigue strength of nickel-based alloy has been widely studied by many studies internationally. In 1997, M. Heilmaier et al from German pointed out that grain structure determines the fracture path, but cannot be correlated with the cyclic lifetimes [3]. In 2002, Weiju Ren et al from American indicated that small fractions of low cycle fatigue life consumption significantly reduce the subsequent high cycle fatigue limit [4]. In 2010, Mao X.P. et al from China paid their attention to the low cycle fatigue strength of Hastelloy C-276 in high temperature [5]. In 2015 Zhang X.C. et al studied the commonly used GH4169's fatigue strength for different grain size [6-7]. And Buckson R.A. from Canada studied the fatigue crack growth rate in Ni-based Hastelloy alloy [8]. By 2016 Wu D.J. et al paid their attention to the welding of Hastelloy C-276, and get the S-N curve of the Hastelloy C-276 weld joint [9-10]. Besides, the importance of weld geometry has also been widely considered. In 2010, A.M. Al-Mukhtar et al from Germany indicated that among different parameters, initial crack length is the most serious factor in fatigue life calculation [11]. In 2011, Zhang X. et al paid their attention to the fatigue crack growth rate in different region [12]. In 2016, Sami Liinalampi studied the influence of actual weld geometry especially some weld defects on stress concentration and fatigue strength [13]. In 2017, Wolfgang F. indicated that the crack don't initiate from corner and weld toe in spite of the high stress peaks, but from adjacent [14]. And Ceferino S. found that radius in undercuts around weld toe is the key factor for stress concentration calculation [15]. In 2018, Liu S. found that a small weld parameter difference can lead to big different in weld geometry and changing the fatigue strength significantly [16]. Few of the previous studies involving fatigue strength of nickel based alloy had paid their attention to the weld joint of Hastelloy C-276 thin sheet. In addition, when it comes to the fatigue strength of weld joints, stress concentration caused by weld toe has drawn much attention. While controlling the reinforcement and weld width have been considered in detail, the weld parameters' influences on fatigue strength by controlling weld geometries were rarely reported. Weld process parameters can determine the distribution of filling metal on top and bottom surface which affect the stress concentration and fatigue strength of weld joints when the thickness of base metal is relatively small.

The present work mainly focused on the effect of weld parameters changes on weld toe flank angle and fatigue strength. Finite element method simulation was conducted to evaluate the fatigue strength of weld joints with different weld geometries by comparing the area of local plastic deformation. A three-factor-three level Box-Behnken design (BBD) experiment of Respond surface method (RSM) is used to determine the relationship between laser input process parameters viz., defocus length (DL), welding speed (WS), feeding speed (FS) over three response i.e., flank angle on top side (FA_{up}), flank angle on bottom side (FA_{down}) and area of local plastic deformation (LPD).

2. Experimental Setup and Methods

2.1. Experiment Setup

The experimental setup is shown in Figure 1. A millisecond pulsed Nd:YAG laser system(GSI LUMONICS) and CNC numerical control machine(JK701H) was applied. And the laser used is 1064-nm wavelength and multimode beam whose focal beam diameter was approximately 0.6 mm. The incident direction of pulsed laser was perpendicular to the substrate surface while the filler wire is fixed at 30°. The argon shielding gas was applied on both top and bottom surface. The top surface shielding gas was delivered through a nozzle with 0.3 MPa pressure for both protecting molten metal from oxidation and enhancing the cooling rate. While the bottom shielding was delivered uniformly on the whole welding seam protecting the molten metal from oxidation. The experiment was conducted on Hastelloy C-276 thin sheet with the thickness of 0.5 mm. The chemical composition of the material is shown in Table 1 which follows the ASME B575 N10276 standard. 0.5 mm diameter ERNiCrMo-4 filler wire was chosen as filling metal whose chemical composition was also shown in Table 1. The substrate surfaces were grinded with 600 grit silicon carbide paper and then cleaned by ethanol to remove the oxide and oil before welding. The typical cross-section morphology of weld joints and commonly analyzed features were shown in Figure 2. The weld width (W) and reinforcement height (H) can be measured. And by simplifying the reinforcement geometry to an arc, the flank angle can be calculated with W and H. The flank angle is the key factor in calculating stress concentration which would raise stress and affect the fatigue strength of weld joint.

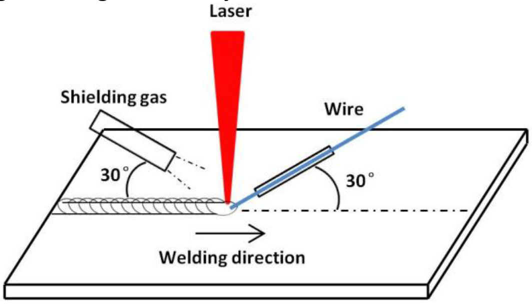

Fig. 1. Experiment setup

Table 1. Chemical composition of Hastelloy C-276 86 and ERNiCrMo-4 (wt %)

Sample	Ni	Fe	Cr	Mo	W	Co	Mn	C	Si	P	S	V
Hastelloy C-276	Bal.	5.14	16.00	15.58	3.45	1.26	0.53	0.001	0.02	0.006	0.003	0.01
ERNiCrMo-4	Bal.	5.30	16.00	15.20	3.30	0.11	0.41	0.009	0.03	0.003	0.001	0.01

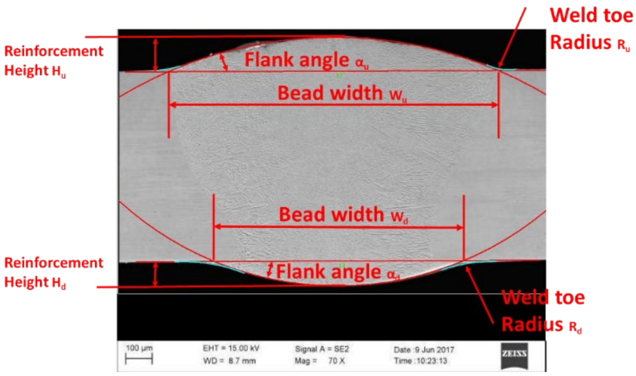

Fig. 2. Cross-section of weld bead of pulsed laser welding with filler wire.

2.2. RSM experiment design

RSM design is an optimization technique which can establish a function relationship between some important input factors and a set of measured responses. It's a statistical and mathematical method which is popular in engineering project. With RSM experiment, it's possible to find the optimal process parameters set and reduce the number of experiments.

Laser welding involve multiple process parameters, including pulse energy, pulse duration, pulse frequency, shielding gas, defocus length, welding speed and feeding speed. Among different parameters, defocus length, welding speed and feeding speed are the most important three parameters. The defocus length (0-2-4 mm) determines the size of laser facula area, which has great influence on weld width. The welding speed (300-350-400 mm/min) determines the linear heat input, which influence the weld penetration depth and weld width significantly. Combining with welding speed, feeding speed (230-290-350 mm/min) can determine the reinforcement geometry. So with help of design-expert software, the RSM experiment was design to evaluate the relationship between 3 process parameter and weld geometry.

3. Results and Discussion

3.1. RSM experiment results

The filling metal during weld process became reinforcement on both side, which is geometric discontinuity leading to stress concentration. Stress concentration would raise the stress around weld toe, where fatigue crack would initiated easier and reduce the fatigue strength. The stress concentration depend on the weld toe flank angle. Weld joint with bigger flank angle would cause severer stress concentration and higher peak stress.

The weld geometries, which obtained from RSM experiment, were measured in Image-Pro Plus. The data was analyzed statically using Design Expert software. And the analysis of variance (ANOVA) method was applied on analyzing the model which include the F-test, coefficient of R^2 and standard derivation. These factors could help illustrate the reliability of respond surface regression model.

The software suggested the flank angle on top surface (FA_{up}) should be presented in quadratic model, and the ANOVA result is given in table 2. Value of Prob>F indicate if the model term is significant. The p-value greater than 0.1 means this model or term is insignificant and may occur due to the noise. While if P-value is less than 0.05 indicate the model or term is significant. According to the table, the model is found to be significant because the p-value is 0.0001, which means there is only 0.01% chance that this model could occur due to the noise. ANOVA results of FA_{up} model shows the terms DL, WS, FS, the interaction terms DL×FS, and the quadratic terms WS^2, FS^2 are significant terms. Lack of fit value describe how well the model fits the experimental data and is desirable to have an insignificant p-value[17].

Table 2. An example of a table

Source	Sum of Squares	df	Mean Square	F Value	p-value Prob > F	
Model	145.13	6.00	24.19	16.15	0.0001	significant
A-DL	9.32	1.00	9.32	6.23	0.0317	
B-WS	71.61	1.00	71.61	47.83	< 0.0001	
C-FS	24.30	1.00	24.30	16.23	0.0024	
AC	9.42	1.00	9.42	6.29	0.0310	
B^2	9.05	1.00	9.05	6.04	0.0338	
C^2	22.93	1.00	22.93	15.32	0.0029	
Residual	14.97	10.00	1.50			
Lack of Fit	13.17	6.00	2.19	4.87	0.0738	not significant
Pure Error	1.80	4.00	0.45			
Cor Total	160.10	16.00				
Std. Dev.	1.223661		R^2	0.906477		
Mean	13.08353		Adj R^2	0.850363		
C.V. %	9.352685		Pred R^2	0.691205		
PRESS	49.4393		Adeq Precision	14.18314		

In Table. 2, some other important factors should also be considered. The coefficient of variation (C.V) is the ratio of the standard error of estimate to the mean value, and is normally considered reasonably reproducible if its value less than 10%. Thus this RSM experiment can be considered as a high precise and reliable experiment. The predicted R^2 is a measure of how good the model predicts a response value, and the difference between it and adjusted R^2 should be less than 0.2. The adequate precision compares the range of predicted value at the design points to the average prediction error which measures the signal to noise ratio. A value greater than 4 indicates an adequate signal, and the model can be used to navigate the design space. The regression equation obtain from the Design Expert Software in terms of actual factors is given below.

$$FA_{up}=7.7547-3.1685\times DL-0.3501\times WS+0.3790\times FS+0.0128\times DL\times FS+0.0006\times WS^2-0.0007\times FS^2$$

Similar data was analyzed for flank angle on bottom side (FA_{down}). ANOVA results showed that the model's p-value is less than 0.0001. All terms, interaction terms and quadratic terms are significant other than A×B and B^2 terms. The lack of fit value is 0.319 which means the lack of fit is not significant relative to the pure error. The experiment is reliable because C.V is 5.1%. The adequate precision is 17.60 which can be used to navigate the design space. And the regression equation obtain from Software in terms of actual factors is given below.

$$FA_{down}=9.2775-7.1002\times DL-0.0499\times WS+0.0758\times FS+0.0200\times DL\times FS+0.0003\times WS\times FS+0.3518\times DL^2-0.0003\times FS^2$$

The ANOVA analysis showed that the RSM experiment is reliable in optimizing the flank angle which has great influence on stress distribution and fatigue strength. So the weld geometry data can be used for Finite element method simulation for studying fatigue strength of weld joints with different weld geometry.

3.2. Finite element method simulation results

The FEM software, ANSYS Workbench, was applied to evaluate the stress distribution during the tension and fatigue loading for different weld joints obtained from RSM experiment. The actual weld joints and FEM model was shown in figure 3.

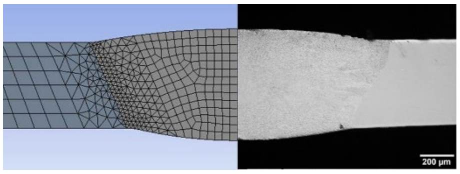

Fig. 3. Finite element model and actual weld geometry

1/4 of the models were used for static stress analysis and fatigue life calculation because of the symmetry. Theoretically the weld toe region had bigger stress than other region because of the stress concentration. So hexahedron element of size 0.1 mm were used in the region away from weld toe to reduce time. And the weld toe region was modeled using tetrahedron elements and pyramid elements of size 0.03 mm for better accuracy. The model and the element were shown in Figure 4. Symmetry constraint was applied on the body symmetric surface marked red. Uniform load of 390 MPa were applied on the end surface where red arrow pointed. The yielding stress of Hastelloy C-276 was 415 MPa, and the S-N curve for weld metal and base metal were from previous work [10].

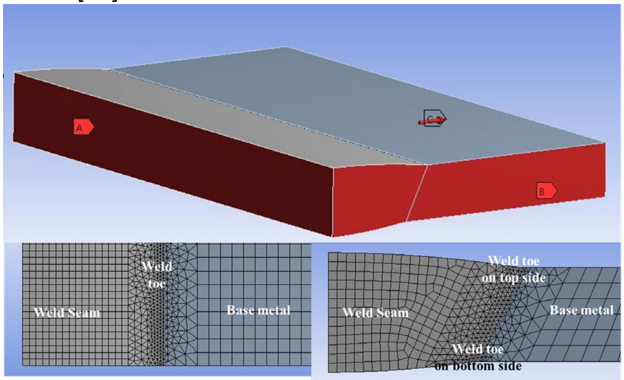

Fig. 3. FEM mesh and boundary condition

The stress distribution of weld joint was shown in figure 4. The peak stresses in different weld joints all located around the weld toe, while their magnitude fluctuated around 416 MPa which didn't change much with the weld geometries. The peak stress exceeded the yielding stress causing the local plastic deformation (LPD), as shown in figure 4(b), which prevent the peak stress from reaching a very high value. The stress concentration raise the stress and the LPD relief the high stress. Two mechanism came to an equilibrium causing that the peak stress maintain stable. LPD may cause the originations of the cracks in high cycle fatigue loading. The risk of fatigue breaks increased with the increasing of the LPD region area around weld toe. The weld width and reinforcement on bottom surface are small compared with those on top surface. Fewer protections was applied on bottom side, so the LPD region occurred mostly around the weld toe on bottom surface.

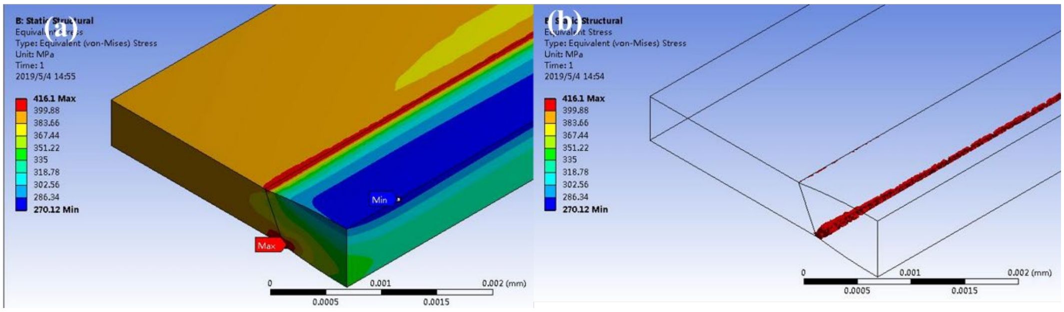

Fig. 4. Stress distribution (a) equivalent stress counter (b) local plastic deformation

Because of the thin thickness, the distribution of filling metal on top and bottom surface would cause great change in stress distribution. The symmetric weld joints' reinforcement heights on both side are close, while the asymmetric weld joints' reinforcement heights on top and bottom side have bigger difference. Comparing the stress distribution of symmetric weld joint and asymmetric weld joint, the area of LPD changed much while the position of LPD did not change. The area of LPD in symmetry weld joints were much smaller because the reinforcement protect both top and bottom side of weld joint and there was no bending torque due to the asymmetry. The area of LPD reach minimum when the weld is totally symmetry in both weld width and reinforcement height.

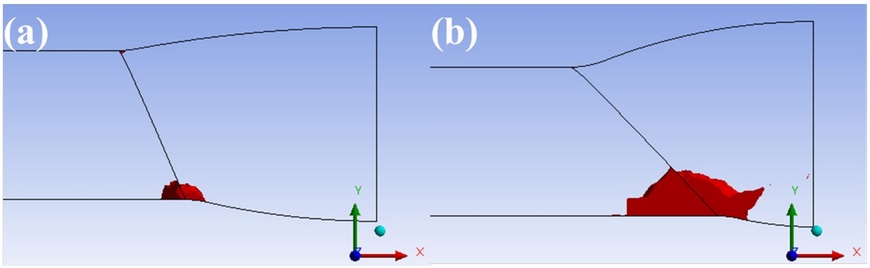

Fig. 4. Local plastic deformation (a) symmetry weld joint (b) asymmetry weld joint

The mechanical properties of base metal and weld metal have small difference, leading to strength mismatch. The stress around fusion line was not continuous, as shown, where the resistance of crack propagation is low. The crack may propagate along fusion line.

3.3. Fatigue strength RSM results

The areas of LPD for different weld joints were measured by Image-Pro Plus software and analyzed by the Design-Expert software. ANOVA results showed that the model's p-value is 0.0255. The interaction terms DL $\times$WS, WS$\times$FS and quadratic term WS^2 are significant terms. The lack of fit value is 0.07. These terms showed that the model is reliable and the change may not occur due to the noise. The modle's prediction error sum of suqares (PRESS) value is 3.113×10^{-3}, which means the model for the experiment is likely to predict the response in a new experiment. The regression equation obtained from software in terms of actual factors is given below.

$$LPD=0.89626-0.033963\times DL-3.78205\times10^{-3}\times WS-1.11974\times10^{-3}FS+9.77604\times10^{-5}\times DL\times WS+2.97528\times10^{-6}\times WS\times FS+3.76726\times10^{-6}\times WS^2$$

Figure 5 showed the interactive effect of 3 weld process parameters. From figure 5(a) it is observed that when WS is low, a higher DL may reduce the LPD. Lower WS would lead to higher heat input, while higher DL can distribute the energy in a larger area, reducing the energy density. The filling metal would not gather in the bottom side causing a higher stress concentration. Similarly, when the WS is high, heat input is likely not enough to form a symmetry weld joint. So a shorter DL is needed to increase the energy density. Therefore, the filling metal would not gather on the top surface. Figure 5(b) showed that DL has little influence on FS. Figure 5(c) showed similar tendency in 5(a). The higher WS with higher FS may cause the filling metal gather on top side because of the low heat input and big amount of filling metal to be melt. A weld joint with filling metal gathering on bottom side may be formed because of the large heat input and small amount of filling metal to be melt when both WS and FS are lower.

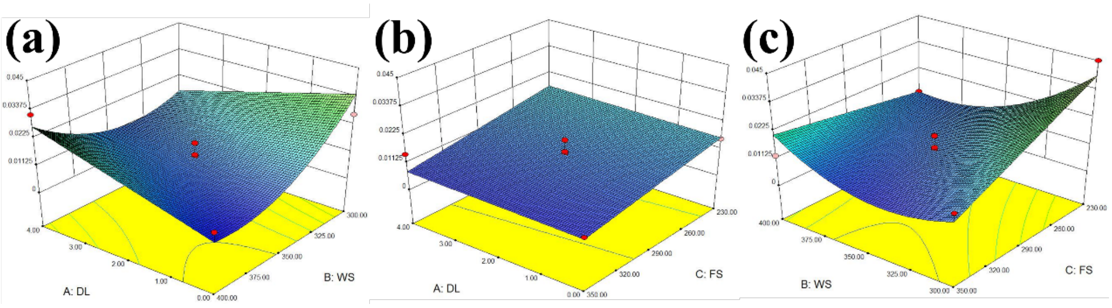

Fig. 5. Interaction plot of weld process parameters (a) DL and WS (b) DL and FS (c) WS and FS

4. Conclusion

This study had established the function relationship between weld process parameters and weld geometry. Based on experimental weld geometry, Finite element method model was built to calculate the stress distribution. Stress concentration and local plastic deformation were taken into consideration to evaluate the fatigue strength of weld joints. Respond surface method regression equation was established between weld parameters and local plastic deformation. The interaction effects of weld parameters were evaluated.

(1) The 3-factor-3-level BBD experiment were conducted to evaluate the influence of weld parameters on weld geometry. The 3 factor are defocus length, welding speed and feeding speed. The flank angle on top and bottom surface were evaluated. The ANOVA results showed that the experiment is precise and significant.

(2) Peak stresses in different weld joints stress distribution did not change with the weld geometry. While the local plastic deformation area changed significantly. The local plastic deformation usually lied around the weld toe on bottom side. The symmetry weld geometry has less local plastic deformation area and would reduce the risk of crack initiation. There is strength mismatch around fusion line which would reduce the resistance of crack propagation.

(3) Regression equation were established between weld parameters and local plastic deformation area. The model is significant according to ANOVA results. Interaction effect of weld parameters were evaluated by Design-Expert software. Welding speed is considered as the most important parameter because it determines the heat input and amount of filling metal. The welding speed has influence on optimization of defocus length and feeding speed.

Acknowledgements

The authors would like to acknowledge the financial support from The National key research and development plan of China (2018YFB1107801, 2018YFB1107802), National Key Basic Research Program of China (No. 2015CB057305), Science Fund for Creative Research Groups of NSFC (No. 51621064)

References

Zhang, Q. , Tang, R. , Yin, K. , Luo, X. , & Zhang, L., 2009. Corrosion behavior of hastelloy c-276 in supercritical water. Corrosion Science, 51(9), 0-2097.

Hashim, M. , Sarath, R. B. K. E. , Duraiselvam, M. , & Natu, H., 2013. Improvement of wear resistance of hastelloy c-276 through laser surface melting. Materials & Design, 46, 546-551.

Müller, F. E. H., Heilmaier, M., & Schultz, L., 1997. The influence of texture and grain structure on the high temperature low-cycle fatigue behaviour of the ODS nickel-based superalloy PM 1000. Materials Science and Engineering: A, 234, 509-512.

Ren, W., & Nicholas, T., 2002. Effects and mechanisms of low cycle fatigue and plastic deformation on subsequent high cycle fatigue limit in nickel-base superalloy Udimet 720. Materials Science and Engineering: A, 332(1-2), 236-248.

Mao, X. P., Lu, D. G., Xu, H., Zhang, L. Y., Wang, G., Xue, F., & Yu, W. W., 2010. Experimental Study on High Temperature Low-cycle Fatigue of Ni-based Alloy C276 Under Strian-controlled With Time Holding. Proceedings of the CSEE, 2010(17), 16.

Qin, C. H., Zhang, X. C., Ye, S., & Tu, S. T., 2015. Grain size effect on multi-scale fatigue crack growth mechanism of Nickel-based alloy GH4169. Engineering Fracture Mechanics, 142, 140-153.

Deng, G. J., Tu, S. T., Zhang, X. C., Wang, Q. Q., & Qin, C. H., 2015. Grain size effect on the small fatigue crack initiation and growth mechanisms of nickel-based superalloy GH4169. Engineering Fracture Mechanics, 134, 433-450.

Buckson, R. A., & Ojo, O. A., 2015. Analysis of the influence of laser welding on fatigue crack growth behavior in a newly developed nickel-base superalloy. Journal of Materials Engineering and Performance, 24(1), 353-361.

Chai, D., Wu, D., Ma, G., Zhou, S., Jin, Z., & Wu, D., 2016. The effects of pulse parameters on weld geometry and microstructure of a pulsed laser welding Ni-base alloy thin sheet with filler wire. Metals, 6(10), 237.

Liu, S., Wu, D.D., Chai, D.S., Zhou, S.Y., Ma, G.Y., Zhou, P., Wu, D.J., 2015. Fatigue property of laser welded joints of Hastelloy C−276 thin sheet, The Chinese Journal of Nonferrous Metals 24,353-361.

Al-Mukhtar, A. M., Biermann, H., Hübner, P., & Henkel, S., 2010. Determination of some parameters for fatigue life in welded joints using fracture mechanics method. Journal of materials engineering and performance, 19(9), 1225-1234.

Zhang, X., & Bao, R., 2011. Evaluation of the intrinsic crack growth rates of weld joints. International Journal of Fatigue, 33(4), 588-596.

Liinalampi, S., Remes, H., Lehto, P., Lillemäe, I., Romanoff, J., & Porter, D., 2016. Fatigue strength analysis of laser-hybrid welds in thin plate considering weld geometry in microscale. International Journal of Fatigue, 87, 143-152.

Fricke, W., Gao, L., & Paetzold, H., 2017. Fatigue assessment of local stresses at fillet welds around plate corners. International Journal of Fatigue, 101, 169-176.

Steimbreger, C., & Chapetti, M. D., 2017. Fatigue strength assessment of butt-welded joints with undercuts. International Journal of Fatigue, 105, 296-304.

Liu, S., Mi, G., Yan, F., Wang, C., & Li, P., 2018. Real weld geometry determining mechanical properties of high power laser welded medium plates. Optics & Laser Technology, 102, 100-110.

Suthakar, T., Balasubramanian, K. R., & Sankaranarayanasamy, K., 2012. Multi objective optimization of laser welding process parameters by desirability approach of design of experiments. In ASME 2012 International Mechanical Engineering Congress and Exposition (pp. 1921-1929). American Society of Mechanical Engineers.